

MORPHOLOGICAL STUDY OF THE PARTICULATE MATTER SAMPLED FROM THE EXHAUST OF A DIESEL ENGINE IN DIESEL AND DUAL FUEL MODES

Nirendra N Mustafi¹, Robert R Raine²

¹Dept. of Mechanical Engineering, Rajshahi University of Engg. and Tech., Rajshahi, Bangladesh

²Dept. of Mechanical Engineering, The University of Auckland, Auckland, New Zealand

ABSTRACT

The particulate matter (PM) of a diesel engine operated on diesel and dual fuel modes are sampled and characterized by size, morphology and fractal geometry by using scanning electron microscopy (SEM) and transmission electron microscopy (TEM). The gaseous fuels used are natural gas and synthetic biogas. The engine operating condition is kept the same to compare the results between diesel and dual fuel PM. SEM images yield PM agglomerate number size distributions and a shape description. TEM images provide the primary particles size distribution in PM agglomerates and the fractal dimensions. Long chainlike PM agglomerates appear for the diesel PM, whereas those for dual fueling are found to be smaller and rounder. All of the measured PM appear to have a bi-modal number size distribution. The average primary particle diameter increases for dual fuel PM (ranging from 26.9 to 29.5 nm) compared to diesel PM (26.4 nm). The average primary particle diameter tends to increase for biogas fueling. Higher fractal dimensions (from 1.73 to 1.88) are obtained for dual fuel PM compared to diesel PM (1.69) implying that diesel PM are more chainlike and elongated. Based on the obtained results, a conceptual model is constructed to understand the phenomena of PM formation for the two types of engine fueling.

Keywords: Dual Fuel Engine, Particulate Matter, Morphology.

1. INTRODUCTION

Diesel engines are efficient and widely used in both stationary and mobile applications. However, diesel engines emit harmful particulate matter (PM). Exposure to diesel PM occurs within many different occupational groups and diesel PM can make an important contribution to ambient PM [1]. Due to their alleged adverse health and environmental effects, diesel PM have been of great concern in recent times.

Gaseous fuels in diesel engines operate in dual fuel mode where the main energy comes from the gaseous fuel and a minimum amount of diesel acts as the ignition source. A diesel engine can easily be modified to dual fueling condition and the engine can switch over either mode of operation under load. Since diesel engine operates at high compression ratios, it permits the use of low energy content gaseous fuels such as biogas. The benefits of using biogas are two fold: substitution for diesel fuel and proper use of green house gas, methane. The use of natural gas in diesel engines is already in practice because of its availability in many parts of the world. Biogas is a renewable fuel, on the other hand, can be produced from organic wastes.

In addition to gravimetric measurements, PM characterization such as number, and size distributions, shape or fractal dimension is also important to provide

better understanding of particle formation and removal processes. The size and structure of PM influence their atmospheric transport properties, optical properties, deposition behavior, depth of penetration into the lung etc. [2-3].

In diesel engine combustion soot particles are formed as a result of incomplete combustion in fuel rich zones and hydrocarbons are adsorbed or condensed onto their surfaces afterwards [4-5]. Numerous research works are available relative to diesel engine PM emissions and their characterization, research gaps remain, in the case of measurements of PM generated by dual fuel engines.

A light duty diesel engine modified to dual fuel operation is used in this research. Electron microscopy techniques have been used to characterize PM physically and to investigate their morphology as used before [2,6,7]. In this study, scanning electron microscopy (SEM) is used to determine the number size distributions, and the shape of the PM sampled from the engine exhaust. The shape of PM is characterized using a shape factor (SF) as described in [7]. Transmission electron microscopy (TEM) is used to investigate the primary particle diameters and the fractal dimensions of the sampled PM agglomerates. Results are compared between diesel and dual fuel conditions. Based on the

above observations, possible growth mechanisms for the PM agglomerates are identified. Finally, a conceptual model has been constructed to differentiate the insights of PM formation processes between the two types of engine fueling.

2. EXPERIMENTAL PARTS

2.1 Engine and Fuels

The investigation was carried out on a Lister Petter, direct injection, diesel engine modified to run in either diesel or dual fuel modes (Table 1). The modification is simple and is described in details in [8-9]. Measurements were taken at two different engine loads: low load (3 Nm) and high load (28 Nm) for diesel fueling and only at high load (28 Nm) for dual fueling. For the dual fueling, the amount of diesel fuel was kept the same as for the diesel low load condition and the desired output torque was obtained by increasing the amount of gas flow into the cylinder. About 62% (by volume) diesel fuel was replaced during dual fueling.

New Zealand low sulfur diesel fuel (~50 ppm sulfur) was used for the experiments. Natural gas (NG) was obtained from the pipeline supply and the detailed composition is provided in [9]. Biogas was prepared by mixing NG with CO₂ in order to obtain different types of biogas: biogas-1 (80% CH₄ and 20% CO₂); biogas-2 (67% CH₄ and 33% CO₂); and biogas-3B (58% CH₄ and 42% CO₂).

2.2 PM Sampling

PM Samples were collected for electron microscopy analysis using a partial flow dilution system with a dilution ratio of ~10:1; further details of the system are provided in [9]. Collected sample filters were preserved in Petri dishes and sealed carefully until microscopy analysis.

2.3 SEM Analysis

For SEM analysis, PM samples were collected on 70 mm Isopore™ polycarbonate membrane filters with 0.4μm pore sizes [10]. These filters have low contrast and very smooth surfaces, which make them suitable for SEM analysis [6]. Prepared samples were examined using a Phillips XL-30S Field Emission Gun. At least 30 SEM images were recorded for each PM sample in this study.

2.4 TEM Analysis

Impaction sampling was used for TEM analysis where the TEM grids holder (a thin perforated strip of “post-it”) is attached onto a gravimetric filter through which the diluted exhaust gas passes the existing partial

Table 1: Engine specifications

Engine type	Single-cylinder, DI, water- cooled
Bore/Stroke	87.3/110 (mm)
Swept volume	659 (cm ³)
Con. rod length	231.9 (mm)
Compression ratio	16.5
Inj. timing by spill	28°bTDC
Engine speed	1750 rpm

flow dilution tunnel system [11]. A CM12 TEM (Philips, FEI Company, Netherlands) was used to examine the PM samples and was operated at an accelerating voltage of 120 kV. TEM images were observed and digitized with the associated image acquisition system equipped with a Model 792 Bioscan digital camera (Gatan Inc., USA) and stored as 1024x1024 pixel computer images. Sufficient images were recorded at both lower and higher magnifications to count about 200 PM agglomerates and at least 300 primary particles respectively for any type of PM sample.

2.5 Image Analysis

Digital images obtained from SEM and TEM examinations were analyzed using public domain image processing software ImageJ, Version 1.38l [12]. ImageJ yielded counting, measurement of projected areas (A_a), perimeters (P), projected area equivalent diameters (D_p), fitted best-fit ellipses and measurement of maximum projected length (L_{max}) and width (W_{max}) of the PM agglomerates. It also provided the means to determine the primary particle diameter (d_p) from agglomerates.

3. RESULTS AND DISCUSSION

3.1 Distribution of Primary Particle Diameters

From the TEM micrographs, primary particles with distinguishable boundaries in the PM agglomerates were selected randomly and their diameters were measured. Results are presented for different engine operating conditions in Fig. 1. The average primary particle diameters, \bar{d}_p , measured for different fueling, range from 25.9 to 29.5 nm, which are in the range of those obtained for light duty diesel particulates in [13].

As the load increases from low to high, during diesel fueling, the combustion temperature as well as the exhaust temperature remains sufficiently high to provide relatively high oxidation rate of the growing PM and thus reduced \bar{d}_p is obtained in the latter case [13-14].

The difference in \bar{d}_p values between diesel high load and dual fuel conditions can be attributed to the combined effects of combustion temperature and duration of combustion. Like high combustion temperature, longer combustion duration can also cause a reduction of the primary particle diameter in diesel high load condition. Higher value of \bar{d}_p for higher CO₂ containing biogases can be speculated as the negative impact on PM oxidation rate due to the presence of high proportion of diluent CO₂ in fuel. Because CO₂ in biogas results in a low flame temperature as well as a low oxygen content inside the cylinder.

3.2 PM Number Size Distribution

SEM images of PM agglomerates were analyzed to yield the projected area equivalent diameter (D_p), which is defined as the diameter of a circle having the equal area of the projected agglomerate. Figure 2 shows the measured PM (agglomerates) number size distribution with fitted bimodal lognormal distributions for different engine operating conditions. A bi-modal number size

distribution is obtained irrespective of type of fueling.

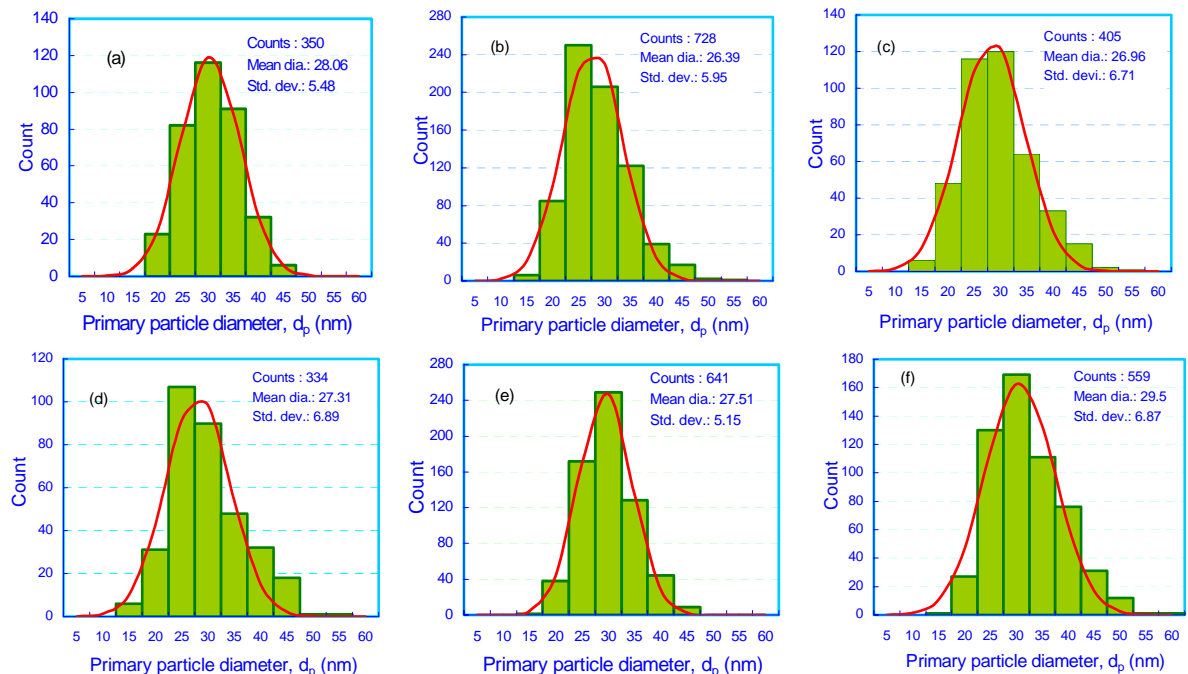


Fig 1. Primary particle size distributions at different engine fueling conditions: (a) diesel low load (3 Nm), (b) diesel high load (28 Nm), (c) diesel-NG (28 Nm), (d) diesel-BG1 (80% CH₄ and 20% CO₂); (28 Nm), (e) diesel-BG2 (67% CH₄ and 33% CO₂); (28 Nm), and (f) diesel-BG3B (58% CH₄ and 42% CO₂); (28 Nm).

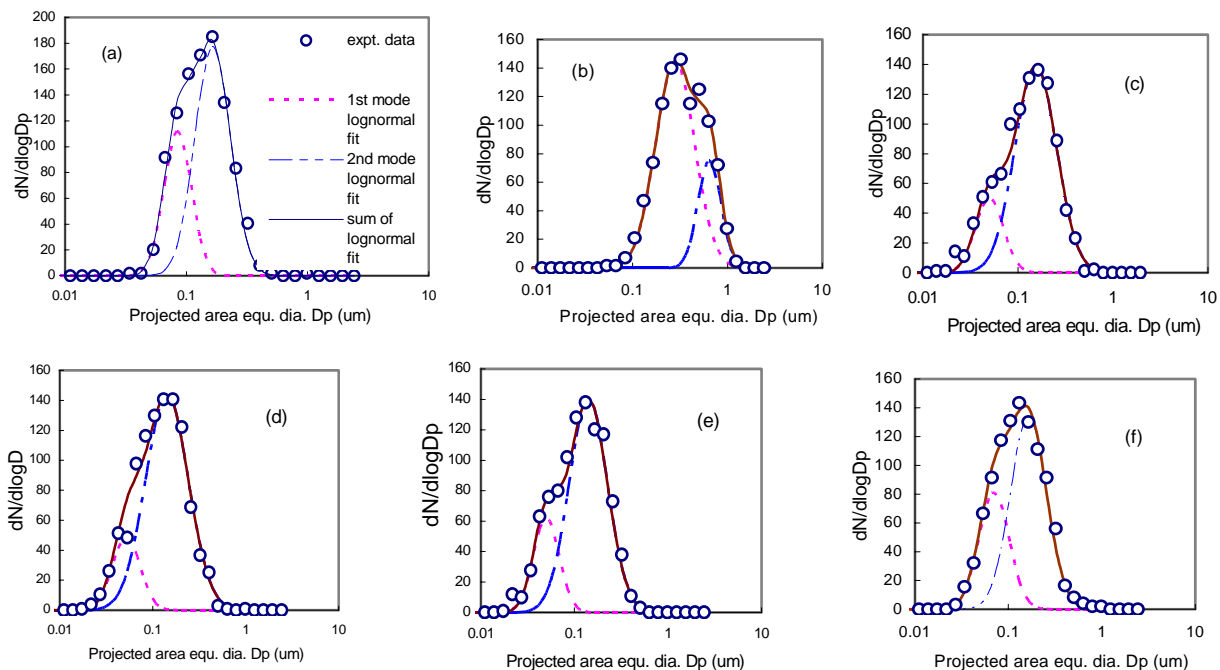


Fig 2.. Number size distribution with fitted bimodal lognormal distribution of the PM agglomerates measured for different engine operating conditions: (a) diesel low load (3 Nm), (b) diesel high load (28 Nm), (c) diesel-NG (28 Nm), (d) diesel-BG1 (80% CH₄ and 20% CO₂); (28 Nm), (e) diesel-BG2 (67% CH₄ and 33% CO₂); (28 Nm), and (f) diesel-BG3B (58% CH₄ and 42% CO₂); (28 Nm). CMD = count median diameter; GSD = geometric standard deviation.

All the measured PM on the SEM filters appear to be in the range of fine particles, $D_p < 2.5 \mu\text{m}$, which are composed of ultrafine particles, $D_p < 0.1 \mu\text{m}$ and nanoparticles $D_p < 0.05 \mu\text{m}$ [5]. It is observed from Fig. 2 that PM agglomerates size measured on SEM filters has mainly 2 modes of distributions: nuclei (D_p less than $0.1 \mu\text{m}$) and accumulation mode ($0.1 < D_p < 1.0 \mu\text{m}$) except the diesel (high) where PM size modes are found to be an accumulation and an almost coarse mode (D_p larger than $1.0 \mu\text{m}$). However, no distinguishable nuclei mode particles are observed for diesel (high) PM. This can be attributed to the fact that a smaller amount of soluble organic fraction (SOF) or volatile fraction (VF) is produced during diesel high load condition as compared to either diesel low load or dual fueling [8], which can contribute to the nuclei mode particles in the exhaust.

The median diameter for dual fueling in nuclei mode region is found to be about $0.05 \mu\text{m}$. The second peak (accumulation mode) of the lognormal fits in Fig. 2 are observed at $D_p = 0.16 \mu\text{m}$ to $0.14 \mu\text{m}$ for diesel low load and dual fuel operation. But for diesel high load condition, the peak of the accumulation mode is observed at $D_p = 0.28 \mu\text{m}$. This indicates that the PM agglomerates measured on SEM filters have significantly larger median diameter for diesel (high) fueling compared to other fueling conditions for the same mode of particles. These results are in good agreement with the previous results reported in [4,15].

3.3 Shape Analysis of the Agglomerates

The shape factor, SF, is used to define the external shape of PM agglomerates appear on SEM filters. This SF is calculated from the minor and major axes of the best-fitted ellipses around PM agglomerates [7]:

$$SF = (\text{minor axis length} / \text{major axis length}) \quad (1)$$

SF is sensitive to particulate elongation. SF close to 1.0, indicates that the particles are nearly spherical and SF close to 0.1 indicates that the particles are long-chained or elongated [7].

Figure 3 presents the shape factor of the measured PM for diesel and dual fueling. Comparing the results between diesel high load and dual fuel PM, a significant difference in the nature of the SF curves is noted. In the case of dual fuel operations, all the peaks are close to 0.7, compared to diesel (high) at about 0.5. This indicates that the PM measured for dual fueling are more nearly spherical compared to diesel (high) fueling.

In the coagulation processes, spherical solid soot particles collide with each other and coalesce and form a larger primary spherical particle. When the rate of particle growth slows down, continued collision between the spherical primary particles results in agglomeration to form large clusters of primary particles, which appear to be chain-like. The rate of agglomeration is proportional to the square of the primary particle number density [16]. The major source of PM formation can be

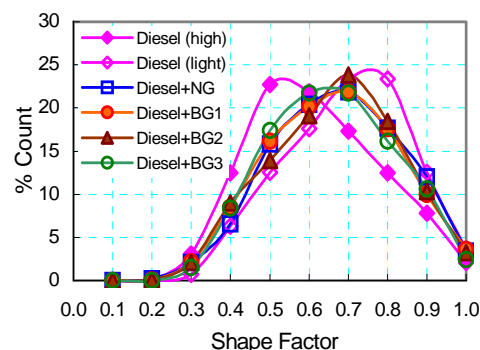


Fig 3. Shape factor (SF) trends of the PM collected on SEM filters for diesel and dual fueling (1750 rpm, and pilot = 0.6 kg/hr for dual fueling).

attributed to the diesel fuel injected into the cylinder. The use of gas during dual fueling is thus expected to produce little PM compared to the diesel (high) as diesel injection is minimized. As number density of the primary particles formed in the case of diesel (high) fueling will be much higher than that for diesel (low) or dual fueling, the corresponding rate of production of agglomerates is also higher in the first case.

3.4 Fractal Morphologies of the Agglomerates

Although the primary particles are nearly spherical, the sizes and shapes of PM agglomerates vary significantly. The complex morphology of the agglomerates can be characterized as fractals. PM fractal dimensions are calculated for the different engine operating conditions. The necessary formula and the associated assumptions used in calculation are presented in the Appendix. Fractal dimension based on maximum projected length (D_{FL}) is used in this study instead of fractal dimension based on radius of gyration (D_f). The two fractal dimensions, D_{FL} and D_f , have identical values and can be used interchangeably [3].

Figure 4 shows an example of the results as a plot of the number of primary particles in an agglomerate, N versus L_{max} / \bar{d}_p on logarithmic scales (where fractal dimension D_{FL} , is represented by the slope). Table 2 presents the fractal dimensions for the PM measured for different engine operating conditions.

It can be observed that the fractal dimension values (D_{FL}) are in the range 1.69 to 1.88 among which 1.72 is for diesel (low) and 1.69 for diesel (high) fueling. Researchers [13,17] measured fractal dimensions of sampled PM in the range of 1.46-1.70 for a light duty diesel engine while the engine was operated at different low to high speeds and loads. These values are relatively lower than the values obtained in the present study. The main reason is that their calculation did not consider the primary particles overlapping which is an obvious case in any agglomerate. Primary particles overlapping [18] was considered in this study to calculate the fractal dimension. Besides this, the engine and the operating conditions were quite different compared to the present study. However, similar trends in values are obtained: a higher fractal dimension at low load and a relatively lower

fractal dimension at high load condition.

When comparing the fractal dimension between diesel and dual fueling (Table 2), a higher value (1.73 to 1.88) is always obtained for the latter case. No published literature has been found to compare our results for dual fuel PM. However, several articles are found where morphology was studied on PM obtained from premixed

Table 2: Fractal dimensions of the PM sampled for different engine fueling conditions.

Engine fueling	Fractal dimension, D_{FL}
diesel low load	1.72
diesel high load	1.69
diesel-NG	1.73
diesel-BG2	1.80
diesel-BG3B	1.84
diesel-BG3A	1.88

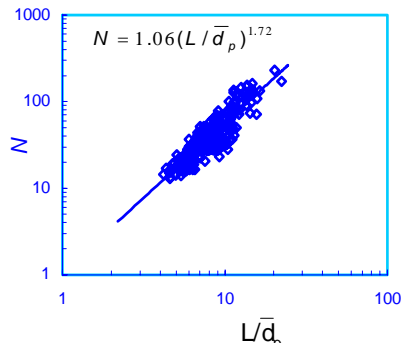


Fig 4. Plot of fractal data of PM agglomerates sampled for diesel low load operation (best fit with $D_{FL} = 1.72$). The number of primary particles per agglomerate N is correlated with the fractal dimension as

$$N = k_L \left(\frac{L_{max}}{\bar{d}_p} \right)^{D_{FL}} ; \text{ While the fractal dimension, } D_{FL}$$

represents the slope, k_L (a correlation prefactor) determines the magnitude of the least-squares linear fit to the data in the $\ln(N)$ versus $\ln(L_{max}/\bar{d}_p)$ plot.

methane/oxygen flames. Fractal dimensions obtained in these studies by light scattering (LS) and TEM methods are in the range of 1.6-1.82. Therefore our results are in the range of previous values but for methane/oxygen premixed flame instead of dual fuel engine environment.

Fractal agglomerates grow through either primary particle-cluster (PC) or cluster-cluster (CC) collisions in three different growth mechanisms: reaction-limited, ballistic and diffusion-limited [19,20]. It can be speculated that at diesel (high) condition, the particulate agglomeration growth is dominated by the diffusion-limited mechanism since the mean free path is generally smaller than the particulate sizes. On the other hand, at dual fuel condition, the growth may be dominated by the ballistic mechanism since the mean free path would be larger than the particulate size, as the parameter, mainly depends on the number concentrations of the particulates [21]. Typically, smaller fractal dimensions indicate more chainlike and larger fractal

dimensions indicate more spherical particulate agglomerates [20]. Thus diesel (high) PM have more chainlike agglomerates than dual fuel PM.

4. CONCEPTUAL MODELING

Based on the results discussed in the previous sections, a conceptual model can be constructed to differentiate the phenomena of PM formation processes for the two types of engine fueling. Figure 5 interprets the phenomenological model of PM formation and oxidation processes for both cases.

Fuel pyrolysis is the starting process where the organic compounds alter their molecular structure at high temperatures but with the presence of negligible amount of oxygen. The pyrolysis process, which results in the production of PM precursors and PM growth species (such as unsaturated hydrocarbons, polyacetylenes, poly aromatic hydrocarbons (PAHs) and especially acetylene), is a function of temperature and fuel concentration [22]. In the case of diesel (high) fueling, the fuel concentration is higher than the dual fueling and therefore pyrolysis process is dominant compared to the oxidation. On the other hand, for dual fueling, the oxidation can be dominant compared to pyrolysis process, as more oxygen is present (premixed combustion) and the diesel fuel quantity is minimized. Since the amount of PM precursors are significantly higher and especially the PAHs are dominant in diesel (high) pyrolysis, a significantly higher particle inception or nucleation is expected in this case compared to dual fueling.

Nucleation is followed by particle surface growth processes where gas phase hydrocarbons (mostly acetylene) are added to the nucleated particles. These particles then combine by colliding with each other. If the collision results in a bigger particle then it is termed as coagulation. The coagulation process results in the appearance of the primary particles. Agglomeration then follows, where primary particles instead of coalescing, stick together and form particulate clusters or chains. The chainlike agglomeration is common in the case of diesel (high) fueling whereas cluster type agglomeration is common in the case of dual fueling. Among the different parameters, the number of primary particles is the dominant parameter enhancing the formation of chainlike agglomerates, which is significantly higher in the case of diesel (high) fueling. It can also be seen from Fig.5 that the amount of gas phase hydrocarbons are significantly higher in the case of dual fueling.

In the dilution system, further PM formation processes can occur as shown in Fig. 5. As the dual fueling results in significantly higher gas phase hydrocarbons (Fig.5), dilution effects are therefore more significant in this case. A substantial amount of both absorption and condensation of the gas phase hydrocarbons would occur in dual fueling. Condensation can cause particle nucleation and thus can cause more fine particles (nucleation mode) to be emitted in this case compared to diesel fueling. This is why the dual fuel PM contains more SOF or volatile matter than the diesel (high) PM [8]. Particle agglomeration can still occur in the dilution system to form more particulate clusters.

It is important to note that the particulate structure for

dual fueling can be approximated to that for diesel (low) fueling. Therefore, it can be speculated that the final structure of the measured PM primarily depends on the quantity of the diesel fuel injected. Every hydrocarbon fuel tends to produce PM on combustion. However, fuel molecules containing less carbon, high hydrogen and straight chain, such as CH_4 , would have a lower tendency to produce PM [22]. Also, the contribution of the oxidation processes in dual fueling is more significant which eventually reduces both the production rate and size of the emitted PM agglomerates.

5. CONCLUSIONS

Based on the above results the following conclusions can be made:

- As the engine load increased from low to high during diesel fueling, the mean primary particle diameter (\bar{d}_p) decreased from 28 nm to 26.4 nm.

The value for dual fueling falls between those for

diesel low load and diesel high load conditions. However, for biogas fueling \bar{d}_p increases from 27.0 to 29.5 nm as CO_2 content increases in biogas.

- All the measured PM agglomerates have a bi-modal number size distribution. Two modes of distributions are: nuclei (D_p less than $0.1 \mu\text{m}$) and accumulation mode ($0.1 < D_p < 1.0 \mu\text{m}$) are observed for all PM except the diesel (high) PM where modes are accumulation and an almost coarse mode (D_p larger than $1.0 \mu\text{m}$).
- According to shape factor analysis, the dual fuel PM agglomerates are nearly spherical and smaller and the diesel (high) PM are larger and elongated.

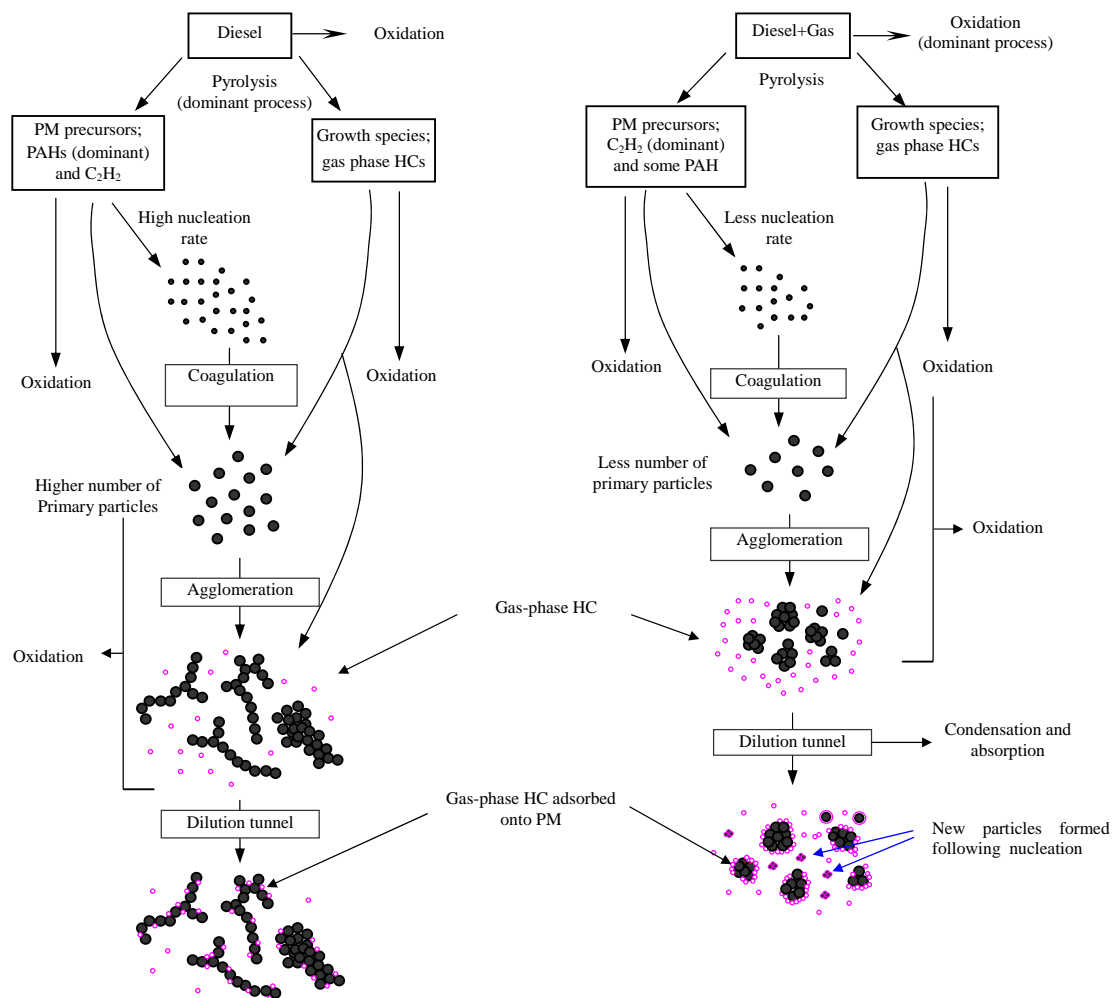


Fig 5. Schematic diagram of the different steps in PM formation process for diesel (high) and dual fueling conditions

Fractal dimension, D_{FL} of the PM agglomerates are found to be in the range of a light duty diesel engine (1.69 to 1.88). For diesel PM, a higher fractal dimension is measured at low load (1.72) than at high load condition (1.69). However, D_{FL} is always higher (1.73 to 1.88) for dual fuel PM compared to diesel (high) PM, indicating more chainlike agglomerates in the latter case.

- The particulate agglomeration growth in the case of diesel fueling may be dominated by diffusion-limited mechanism while that for dual fueling may be dominated by the ballistic mechanism.
- Based on these results a conceptual model of PM formation processes in dual fueling condition in comparison to diesel fueling condition can be constructed.

6. REFERENCES

1. Vouitsis, E., Ntziachristos, L. and Samaras, Z., 2003, "Particulate matter mass measurements for low emitting diesel powered vehicles: What's next?" *Progress in Energy and Combust. Sci.*, 29:635-672.
2. Park, K., Kittelson, D. B. and McMurry, P. H., 2004, "Structural properties of diesel exhaust particles measured by transmission electron microscopy (TEM): Relationships to particle mass and mobility", *Aerosol Sci. Technol.* 38:881- 889.
3. Chakrabarty, R.K., Moosmüller, H., Arnott, W.P., Garro, M.A. and Walker, J., 2006, "Structural and fractal properties of particles emitted from spark ignition engines", *Environ. Sci. Technol.*, 40:6647-6654.
4. Figler, B., Sahle, W., Krantz, S. and Ulfvarson, U., 1996, "Diesel exhaust quantification by scanning electron microscope with special emphasis on particulate size distribution", *The Science of the Total Environ.*, 193:77-83.
5. Kittelson, D.B., 1998, "Engines and nanoparticles: A review", *J. of Aerosol Science*, 29:575-588.
6. Hinds, W. C., 1999, *Aerosol Technology, Properties, Behavior, and Measurement of Airborne Particles*, John Wiley and Sons, Inc., New York.
7. Nord, K., Haupt, D., Ahlvik, P. and Egeback, K-E., 2004, "Particulate emissions from an ethanol fueled heavy-duty diesel engine equipped with EGR, catalyst and DPF", *SAE Paper 2004-01-1987*.
8. Mustafi, N.N., 2008, "Particulate emissions of a dual fuel engine", PhD Thesis, The University of Auckland, Auckland, New Zealand.
9. Mustafi, N.N. and Raine, R.R., 2008, "A Study of the emissions of a dual fuel engine operating with alternative gaseous fuels", *SAE Paper 2008-01-1394*.
10. Mustafi, N.N., Raine, R.R. and James, B., 2007, "Particulate emissions from a diesel engine operated with gaseous fuels", *Proc. of the conference, Chemeca*, Melbourne, Australia.
11. Mathis, U., Mohr, M., Kaegi, R., Bertola, A. and Boulouchos, K., 2005, "Influence of diesel engine combustion parameters on primary soot particle diameter", *Environ. Sci. Technol.*, 39:1887-1892.
12. Rasband, W.S., 1997-2007, *ImageJ*, U. S. National Institutes of Health, Bethesda, Maryland, USA, Available on the internet at <http://rsb.info.nih.gov/ij/>.
13. Zhu, J., Lee, K. O., Yozgatligil, A. and Choi, M. Y., 2005, "Effects of engine operating conditions on morphology, microstructure, and fractal geometry of light-duty diesel engine particulates", *Proc. of the Combustion Institute*, 30:2781-2789.
14. Jung, H., Kittelson, D.B. and Zachariah, M.R., 2004, "Kinetics and visualization of soot oxidation using, transmission electron microscopy", *Combustion and Flame* 136:445-456.
15. Lapuerta, M., Armas, O. and Gomez, A., 2003, "Diesel particle size distribution estimation from digital image analysis", *Aerosol Sci. Technol.* 37:369-381.
16. Smith, O.I., 1981, "Fundamentals of soot formation in flames with application to diesel engine particulate emissions", *Progress in Energy and Combust. Sci.*, 7:275-291.
17. Lee, K. O., Zhu, J., Ciatti, S., Yozgatligil, A. and Choi, M. Y., 2003, "Sizes, graphitic structures and fractal geometry of light-duty diesel engine particulates", *SAE Paper 2003-01-3169*.
18. Oh C. and Sorensen C.M., 1997, "The effect of overlap between monomers on the determination of fractal cluster morphology", *Journal of Colloid and Interface Science*, 193:17-25.
19. Schaefer, D.W. and Hurd, A.J., 1990, "Growth and structure of combustion aerosols: fumed silica", *Aerosol Sci. Technol.*, 12:876-890.
20. Lee, K.O., Cole, R., Sekar, R., Choi, M.Y., Kang, J.S., Bae, C.S. and Shin, H.D., 2002, "Morphological investigation of the microstructure, dimensions, and fractal geometry of diesel particulates", *Proc. of the Combustion Institute*, 29:647- 653.
21. Bird, R.B., Stewart, W.E. and Lightfoot, E.N., 1960, *Transport Phenomena*, John Wiley, New York.
22. Tree D.R. and Svensson K.I., 2007, "Soot processes in compression ignition engines", *Progress in Energy and Combustion Science*, 33:272-309.

APPENDIX

Pm Fractal Dimension

The number of primary particles per agglomerate, N , scales with the overall size of the agglomerate, usually quantified by its radius of gyration, R_g , with a power D_f as described by ([A1-A5]):

$$N = k_f \left(\frac{2R_g}{\bar{d}_p} \right)^{D_f} \quad (A1)$$

where \bar{d}_p is the primary particle diameter, D_f is the fractal dimension, and k_f is the prefactor of the scaling relationship and both D_f and k_f are dimensionless quantities. The primary particle diameter, \bar{d}_p , normally enters into the equation as an average value, \bar{d}_p .

Equation A1 is applicable to an ensemble of agglomerates on the average, i.e. it is statistical in nature [A1]. Essentially, the fractal dimension explains under what mechanism particulate agglomerates are formed and their growth [A6]. The fractal dimension D_f is generally obtained by evaluating the gradient of a linear regression line fit with the data plot of $\ln(N)$ versus $\ln(2R_g/\bar{d}_p)$. The number of primary particles, N , is related to the projected area of the agglomerates as [A2]:

$$N = k_a \left(\frac{A_c}{A_p} \right)^\alpha \quad (A2)$$

where A_c is the projected area of the agglomerate, A_p is the average projected area of the primary particles, k_a is an empirical constant and α is an empirical exponent.

The estimation of N using Eq. A2 is also sensitive to the amount of overlap of any two adjacent primary particles. N is estimated using Eq. A2 with consideration of particle overlap in the present study. The values of k_a and α are obtained from [A2]: for diesel (high) fueling $k_a \sim 1.25$ and $\alpha \sim 1.09$ and for the other types of fueling $k_a \sim 1.35$ and $\alpha \sim 1.1$.

Once N is obtained, the other three-dimensional parameter, R_g , in Eq. A1 is to be determined. The radius of gyration R_g , can actually be estimated from the projected properties of the agglomerates. The fractal dimension is estimated using a characteristic dimension of the agglomerate, maximum length L_{max} , (instead of R_g) as suggested in [A1,A3-A4]. Hence the outer radius of an agglomerate ($R_L \cong L_{max}/2$) can be used in the

determination of D_f and the Eq. A2 can be modified as

$$N = k_L \left(\frac{2R_L}{\bar{d}_p} \right)^{D_{fL}} \Rightarrow N = k_L \left(\frac{L_{max}}{\bar{d}_p} \right)^{D_{fL}} \quad (A3)$$

While D_{fL} represents the slope, k_L (a correlation prefactor) determines the magnitude of the least square linear fit to the data in the $\ln(N)$ versus $\ln(L_{max}/\bar{d}_p)$ plot. The two fractal dimensions D_{fL} (based on maximum projected length) and D_f (based on radius of gyration) have identical values and can be used interchangeably [A7]. However, the proportionality constants k_L and the prefactor k_f are different.

REFERENCES

- A1. Koylu, U.O., Xing, Y. and Rosner, D.E., 1995, "Fractal morphology analysis of combustion generated aggregates using angular light scattering and electron microscope images", *Langmuir*, 11:4848-4854.
- A2. Oh, C. and Sorensen, C.M., 1997, "The effect of overlap between monomers on the determination of fractal cluster morphology", *J. of Colloid and Interface Science*, 193:17-25.
- A3. Park, K., Kittelson, D. B. and McMurry, P. H., 2004, "Structural properties of diesel exhaust particles measured by transmission electron microscopy (TEM): Relationships to particle mass and mobility", *Aerosol Science and Technology*, 38:881- 889.
- A4. Neer, A, and Koylu, U. O., 2006, "Effect of operating conditions on the size, morphology, and concentration of submicrometer particulates emitted from a diesel engine", *Combustion and Flame*, 146:142-154.
- A5. Song, J. and Lee, K.O., 2007, "Fuel property impacts on diesel particulate morphology, nanostructures, and NOx emissions", *SAE Paper 2007-01-01239*.
- A6. Lee, K.O., Cole, R., Sekar, R., Choi, M.Y., Kang, J.S., Bae, C.S. and Shin, H.D., 2002, "Morphological investigation of the microstructure, dimensions, and fractal geometry of diesel particulates", *Proceedings of the Combustion Institute*, 29:647- 653.
- A7. Chakrabarty, R.K., Moosmuller, H., Arnott, W.P., Garro, M.A. and Walker, J., 2006, "Structural and fractal properties of particles emitted from spark ignition engines", *Environmental Science and Technology*, 40:6647-6654.